



Data-driven feedforward control of inertial dampers for accuracy improvement

Kaan Bahtiyar^a, Burak Sencer (2)^{a,b,*}, Xavier Beudaert (2)^b

^a Oregon State University, Corvallis, USA

^b IDEKO, Dynamics & Control Department, Elgoibar, Basque Country, Spain

ARTICLE INFO

Article history:

Available online 22 May 2024

Keywords:

Vibration
Active damping
Learning

ABSTRACT

This paper presents a novel control strategy to minimize residual vibrations and overshoot using inertial dampers in repetitive tasks. In this work, vibration data collected during repeating task is utilized to generate a fully pre-scheduled feedforward compensation signal that assists the inertial damper's original feedback controller to further enhance its vibration mitigation capability. Optimal feedforward signal is determined iteratively over successive operations considering the actuator stroke and force limits. Numerical and experimental results validate the approach demonstrating significant (up to 87%) reduction in peak vibration while using equal or less actuator force as compared to the conventional control.

© 2024 CIRP. Published by Elsevier Ltd. All rights reserved.

1. Introduction

Machine tools and industrial robots frequently perform repetitive tasks in mass manufacturing such as repetitive cutting, welding or material handling. Productivity increase is often limited by residual vibrations induced by the inertial forced vibrations triggered due to rapid motions of the machine axes. Approaches such as trajectory pre-filtering using B-Splines [1], servo tracking error pre-compensation [2], input shaping, or Finite Impulse Response (FIR) filtering based command generation [3] have been proposed to avoid inertial forced vibrations while maintaining the contour accuracy of the machine tool. However, these trajectory generation solutions face practical challenges in industrial settings, primarily due to the limited access to CNC interpolators.

Closed-loop control techniques employing additional acceleration feedback sensors [4] or relying on the internal machine sensors [5] have been proposed to enhance machine tool's accuracy. High-accuracy contouring control can also be achieved through model-reference feedforward (FF) controllers [6]. Such techniques use the known machine dynamics, but they do not benefit from the repetitive nature of the task.

When the task characteristics are not varying from iteration to iteration, batch-to-batch feedforward control [7] and Iterative Learning Control (ILC) have shown promising results, particularly in reducing vibrations in robotic arms [8]. However, these methods also often necessitate substantial modifications to machine controllers, a barrier in many industrial applications.

To circumvent modification of the trajectory generation or the closed-loop control functions of the CNC system, external hardware solutions such as mounting of passive or active dampers on the machine structure are considered to improve machine's dynamic characteristics. Active dampers have been effectively employed in forced vibration reduction [9] and chatter suppression [10] with automated solutions for tuning their feedback control laws [11]. Direct velocity feedback (DVF), implemented with accelerometers, is generally favored for its simplicity and robustness

in inertial damper control. Both DVF and H-inf control laws aims at injecting viscous damping to a targeted mode and have been compared for chatter suppression applications [12]. Additional damping provided by the inertial damper greatly shortens the settling time; however, it does not significantly reduce the initial overshoot. Specific passive mass damper tuning strategies have been proposed for pulse-like responses to further minimize the initial overshoot [13,14], but it has not been yet proposed for inertial actuators.

This paper presents a novel strategy to enable the use of active inertial dampers for effectively suppressing inertial forced vibrations. The idea is to exploit the nature of repetitive cutting, welding or pick-and-place operations, and generate a task-specific pre-scheduled control signal, referred as the feedforward (FF) compensation signal, for the damper to greatly enhance its performance. Fig. 1 illustrates the strategy. Vibration data measured during an operation (task) is used to generate a feedforward compensation signal, which is commanded to the damper in the subsequent task. The response is recorded, and the control signal is iteratively optimized to improve the response over successive tasks while considering the actuator force and stroke limits. The proposed strategy does not require direct communication with the NC system retaining the plug-and-play functionality of the active damper systems.

2. Iteratively tuned compensation signal generation

Let us consider a finite-time repeating task, such as a repetitive cutting, welding or pick-and-place operation where inertial forced vibrations are triggered by the rapid motion of machine tool axes, x_r . As depicted in Fig. 2a-b, when an inertial damper is attached, the target point's motion (vibration) x_t , and the damper mass' relative motion x_d can be modeled as:

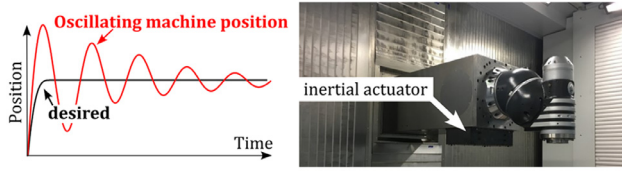
$$\left. \begin{aligned} x_t &= G_{TR}x_r + G_{TF}u_{ff} \\ x_d &= G_{DR}x_r + G_{DF}u_{ff} \end{aligned} \right\} \quad (1)$$

where G_{TR} and G_{DR} denote the dynamics between the target point x_t and machine axis x_r and the damper x_d , respectively. Similarly, G_{TF} and G_{DF} denote the response dynamics due to the FF control (compensation) signal

* Corresponding author.

E-mail address: burak.sencer@oregonstate.edu (B. Sencer).

a) Inertial actuator application for accuracy improvement



b) Iteration-domain block diagram

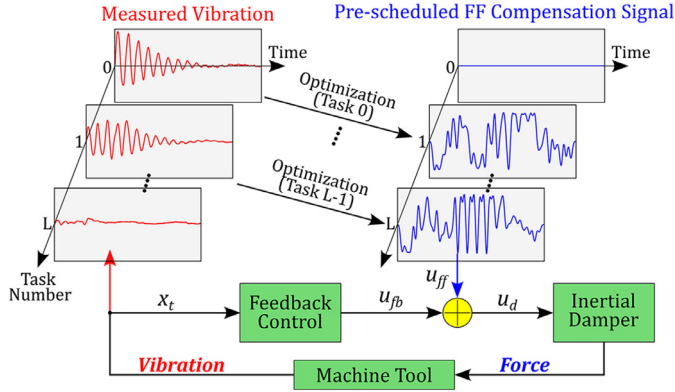
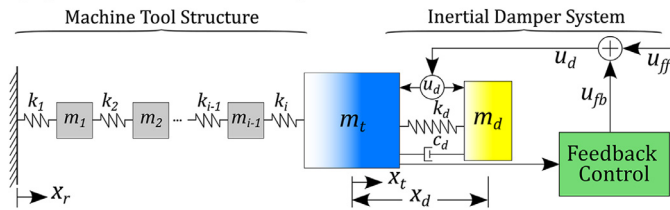
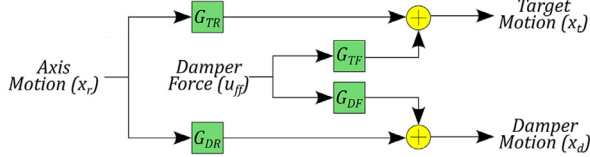


Fig. 1. Iterative compensation scheme for inertial damper.

a) Dynamics with inertial damper



b) Block diagram



c) B-spline signal representation

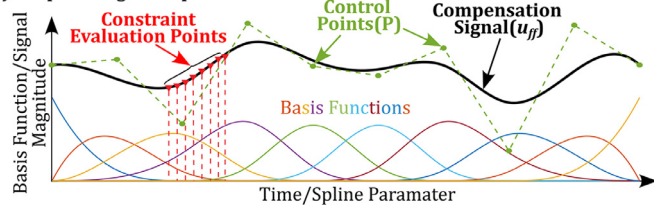


Fig. 2. System model and B-spline signal parameterization.

u_{ff} commanded to the damper's controller. Note that x_r , G_{TR} and G_{DR} are not accessible in practice unless there is a high-fidelity communication with the host CNC. x_t can be measured by a displacement or accelerometer sensor, and G_{TF} and G_{DF} can be identified via a sine-sweep using the inertial damper.

Considering sampled signals during successive tasks; $x_t^{(l)} = [x_t(0) \dots x_t(N)]^T$ denotes vibration recorded during the l^{th} operation (task). The objective is to generate a fully pre-scheduled FF compensation signal $u_{ff}^{(l)}$ for the damper to minimize vibrations either during the entire operation, or at a specified portion of the task. To reduce the number of variables, $u_{ff}^{(l)} = [u_{ff}(0) \dots u_{ff}(N)]^T$ can be parameterized by a smooth B-spline of degree n having $M < N$ control points P as:

$$\begin{bmatrix} u_{ff}(0) \\ u_{ff}(1) \\ \vdots \\ u_{ff}(N) \end{bmatrix} = \begin{bmatrix} N_{0,n}(\zeta_0) & N_{1,n}(\zeta_0) & \dots & N_{M,n}(\zeta_0) \\ N_{0,n}(\zeta_1) & N_{1,n}(\zeta_1) & \dots & N_{M,n}(\zeta_1) \\ \vdots & \vdots & \ddots & \vdots \\ N_{0,n}(\zeta_N) & N_{1,n}(\zeta_N) & \dots & N_{M,n}(\zeta_N) \end{bmatrix} \begin{bmatrix} P_0 \\ P_1 \\ \vdots \\ P_M \end{bmatrix} \quad (2)$$

where ζ represents the B-spline parameter within the range $[0,1]$, effectively normalizing time as a uniformly discretized variable across $N + 1$ points $(\zeta_0, \zeta_1, \dots, \zeta_N)$. $N_{M,n}(\zeta)$ are the B-spline basis functions of choice, evaluated on a uniform knot vector.

Eq. (1) can be re-written using Eq. (2) in lifted domain (vector-matrix form) as:

$$\begin{cases} x_t = G_{TR}x_r + G_{TF}BP \\ x_d = G_{DR}x_r + G_{DF}BP \end{cases} \quad (3)$$

where G_{TR} , G_{DR} are $(N + 1) \times (N + 1)$ convolution matrices containing the impulse response coefficients of G_{TR} and G_{DR} . Also note that the $G_{TF}B$ and $G_{DF}B$ terms in Eq. (3) represent the so-called filtered B-spline basis function [1] matrices.

The objective is to determine the B-spline control points P that define the compensation signal $u_{ff}^{(l)}$ to minimize the target's relative vibration from a set-point $e_t = x_t - x_{set}$ iteratively over successive tasks (operations). This problem can be postulated as:

$$\min_P \left(J = \frac{1}{2} \| e_t \|^2 \right) = \min_P \left(\frac{1}{2} e_t^T e_t \right), \quad (4)$$

and assuming that both the task and the setpoint do not vary $x_r^{(l+1)} = x_r^{(l)}$ and $x_{set}^{(l+1)} = x_{set}^{(l)}$, the B-spline control points P can be determined iteratively over successive tasks by using Newton's iterations without knowing the reference trajectory x_r as:

$$\begin{bmatrix} P_0 \\ \vdots \\ P_M \end{bmatrix}^{(l+1)} = \begin{bmatrix} P_0 \\ \vdots \\ P_M \end{bmatrix}^{(l)} - \alpha (\nabla^2 J^{(l)})^{-1} (\nabla J^{(l)}) \quad (5)$$

where $\nabla J^{(l)}$ is the gradient, and $\nabla^2 J^{(l)}$ is the hessian of the cost function computed based on the signals and measured dynamics:

$$\begin{cases} \nabla J^{(l)} = \frac{\delta J}{\delta P} = \nabla e_t^{(l)T} e_t^{(l)} = (G_{TF}B)^T e_t^{(l)} \\ \nabla^2 J^{(l)} = \nabla e_t^{(l)T} \nabla e_t^{(l)} = (G_{TF}B)^T (G_{TF}B) \end{cases} \quad (6)$$

Notice that $G_{TF}B$ is fixed since it is based on the damper's transmission dynamics and the initial B-spline parameterization. Therefore, the gradient $\nabla J^{(l)}$ is updated after each task (iteration) based only on the recorded vibration data $e_t^{(l)}$, whereas the hessian $\nabla^2 J$ is model-based and constant yielding convex optimization to deliver a globally optimal set of control points P as $l \rightarrow \infty$. α in Eq. (5) is the step-size or also called as the learning gain. Range of learning gains for iteration stability can be analyzed [7] where $1 > \alpha > 0$ provides reliable convergence.

Inertial actuators must operate safely within their stroke and force limits, and hence the above problem (Eq. (4)) is augmented with inequality constraints to generate a bounded control signal:

$$\min_P \left(J = \frac{1}{2} \| e_t \|^2 \right), \text{ subject to: } \begin{cases} u_{LB} \leq u_d \leq u_{UB} \\ x_{LB} \leq x_d \leq x_{UB} \end{cases} \quad (7)$$

where (x_{LB}, x_{UB}) and (u_{LB}, u_{UB}) denote damper's stroke and total force ($u_d = u_{fb} + u_{ff}$) bounds, respectively. This requires the control point increment over successive iterations to be constrained. Vibration propagation can be represented by Taylor approximation as:

$$e_t^{(l+1)} = e_t^{(l)} + \nabla e_t^{(l)T} (P^{(l+1)} - P^{(l)}) + \frac{\nabla^2 e_t^{(l)}}{2!} (P^{(l+1)} - P^{(l)})^2 + \dots \quad (8)$$

where $\nabla e_t^{(l)} = (G_{TF}B)^T$, and $\Delta P^{(l)}$ is the control point increment. Enforcing 1-step convergence by considering only the 1st order term in Eq. (8) yields:

$$e_t^{(l+1)} = 0 \Rightarrow e_t^{(l)} + \nabla e_t^{(l)T} \Delta P^{(l)} = 0, \quad (9)$$

and the optimization problem is re-postulated to enforce Eq.(9) in the sense of least squares with constraints as:

$$\min_{\Delta P^{(l)}} \left(J = \frac{1}{2} \| e_t^{(l)} + \nabla e_t^{(l)T} \Delta P^{(l)} \|^2 \right) \text{ s.t. : } \begin{cases} u_{LB} \leq u_d \leq u_{UB} \\ x_{LB} \leq x_d \leq x_{UB} \end{cases} \quad (10)$$

to determine the optimal control point increment $\Delta P^{(l)}$. The inequality constraints are imposed discretely at m points along the task trajectory as illustrated in Fig. 2c. Since $\nabla e_t^{(l)}$ is constant, the objective function in Eq. (10) is updated based only on the measured vibration $e_t^{(l)}$ at each iteration (task), and the above problem can be solved conveniently using quadratic or linear programming strategies by implementing the constraints linearly as described below:

Step 1: Set trial number $l = 0$, and initialize the FF signal, $u_{ff}^{(0)} = 0$.

Step 2: Execute the task, and measure relative vibration $e_t^{(l)}$, damper's displacement $x_d^{(l)}$ and total force command $u_d^{(l)}$.

Step 3: Evaluate the objective function in Eq. (4) and the actuator limits constraints from Eq. (7). If they are not satisfactory, continue to Step 4. Otherwise, proceed with Step 5.

Step 4: Solve the constrained least squares problem in Eq. (10) by imposing the constraints linearly as:

$$\begin{cases} u_{LB} \leq u_d \leq u_{UB} \\ x_{LB} \leq x_d \leq x_{UB} \end{cases} \rightarrow \begin{cases} u_{LB} \leq u_d^{(l)} + \mathbf{B}\Delta\mathbf{P}^{(l)} \leq u_{UB} \\ x_{LB} \leq x_d^{(l)} + \mathbf{G}_{DF}\mathbf{B}\Delta\mathbf{P}^{(l)} \leq x_{UB} \end{cases} \quad (11)$$

and determine the optimal control increment $\Delta\mathbf{P}^{(l)}$ to generate the FF compensation signal, $u_{FF}^{(l+1)} = \mathbf{B}(\mathbf{P}^{(l)} + \Delta\mathbf{P}^{(l)})$.

Step 5: Increment task number $l \leftarrow l + 1$, and proceed with Step 2.

Remarks: Some remarks can be made on the practical implementation of the proposed algorithm.

- 1) If the damper is used for minimizing structural, e.g. machine frame, column, etc. vibrations, the set-point is typically $x_{set} = 0$. When used for minimizing servo positioning errors, the set-point is selected based on the application such as $x_{set} = x_r$, or it is constructed from the filtered motion signal, x_t .
- 2) The FF signal is finite-time and task-specific, tuned iteratively over repeated execution of the same task.
- 3) To synchronize the FF signal with the task, a trigger is used, which is the only required interaction with the machine's CNC. Alternatively, this could be replaced with an external short-range position sensor to have an independent integration.
- 4) Lastly, the measurement of target point's vibration and damper's displacement require external sensors, e.g. accelerometer or a displacement pick-up. However, once the data-driven FF signal tuning is completed, such signals are no longer needed, and the sensors can be removed.

3. Illustrative examples

Illustrative examples simulate the functionality of the algorithm on the system described in Fig. 3a with the parameters given in Table 1. It resembles a flexible servo mechanism where the load-mass is attached to a rigid wall (motor) and positioned (x_r) back-and-forth repeatedly. A Direct Velocity Feedback (DVF) control is implemented on the active inertial damper to dampen the vibration of the load-mass x_t . Fig. 3b illustrates that the inertial damper can increase the modal damping of the load mass by 5x.

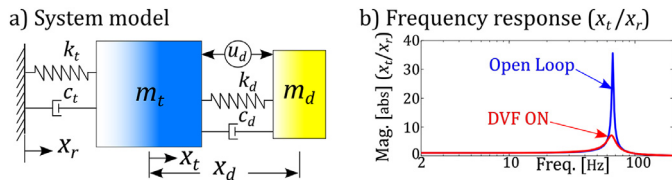


Fig. 3. Single degree of freedom model for illustrative examples.

Table 1
Simulation system parameters.

Mass	Viscous damping	Stiffness	B-spline parameters
$m_t = 50$ [kg]	$c_t = 50$ [Ns/m]	$k_t = 9.6 \times 10^6$ [N/m]	$n = 3$
$m_d = 5$ [kg]	$c_d = 628.3$ [Ns/m]	$k_d = 1.97 \times 10^4$ [N/m]	$M = 500$

The motion command (x_r) planned using a jerk-limited trajectory to travel back-and-forth $L = 40$ mm at a speed of $F = 120$ mm/s, acceleration $A = 3000$ mm/s² and jerk $J = 6 \times 10^5$ mm/s³ shown in Fig. 4a is commanded to the system repeatedly. The objective is to generate the compensation signal for the inertial actuator so that the load-mass m_t does not vibrate relative to the motor position. In this case the set-point becomes the reference trajectory itself $x_{set} = x_r$, and the constrained optimization problem in Eq. (10) is solved.

To ensure a fair comparison, the actuator force and displacement bounds are set identical to the peak values observed when the DVF controlled damper was operating, and the constraints are imposed evenly

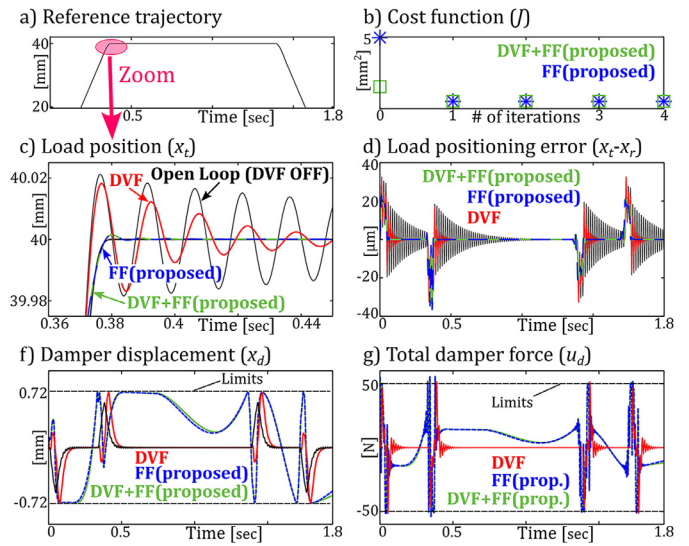


Fig. 4. Illustrative example I.

along the entire trajectory at $m = 1000$ discrete locations. As shown in Fig. 4, the DVF controlled damper helps improve the settling time. However, it cannot eliminate the initial overshoot observed at the motion reversal point of the trajectory (see Fig. 4c). The proposed FF compensation strategy converges after the same task is executed 2 times (See Fig. 4b), and it enables the damper to almost fully eliminate the overshoot as shown in Fig. 4c. The peak overshoot reduces by 93% from $\mp 21\mu\text{m}$ to $\mp 1.4\mu\text{m}$. Notice that the proposed compensation scheme can be implemented to supplement the existing DVF control (See DVF+FF signal in Fig. 4c), or it can be used directly when the damper is operating in open loop (See FF signal in Fig. 4c). The RMS error of Fig. 4d is reduced by 37%. Furthermore, as shown in Figs. 4f-g, damper stroke and force limits are kept unchanged from when DVF was operational.

In practice, x_r cannot be acquired from the NC controller of the host system. x_t can be measured using an accelerometer along the entire trajectory. However, in point-to-point positioning operations, vibrations need to be minimized only at the end/reversal point of the trajectory. Therefore, a displacement sensor with limited range can be used to measure x_t in the vicinity of the motion reversal point, $x_t \in [L \mp \Delta x]$, and the algorithm can be used to minimize vibrations locally around it. During the first task x_t is recorded locally at the trajectory reversal point, and the B-spline control points are allocated in its vicinity. Next, the set-point deviation (e) is locally constructed using a small portion of x_t to minimize its deviation from the reversal-position L as shown in Fig. 5a. $\Delta x = 6$ mm is used, and results are summarized in Fig. 5.

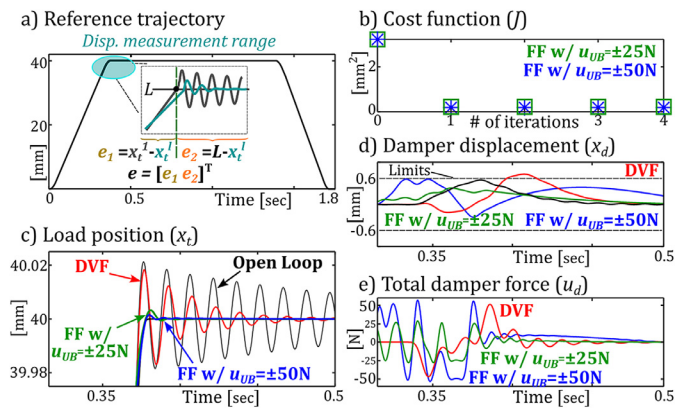


Fig. 5. Illustrative example II.

As shown, even if the algorithm is used to minimize vibrations locally, the overshoot is almost fully eliminated. Furthermore, when reducing vibrations locally, the damper can be commanded to use less force and displacement as compared to the DVF as shown in Figs. 5d) and e). For instance, when the FF signal is constrained to use half of the force level of

DVF control ($50/2 = 25\text{N}$), peak vibration can still be reduced by 85% from $21\mu\text{m}$ down to $3.2\mu\text{m}$. In other words, the inertial damper controlled by the pre-scheduled task-specific FF control signal can outperform the DVF control with less actuator force leading to potentially more compact and cheaper active damper designs.

4. Experimental results

Experiments are conducted on a single axis flexible feed drive system shown in Fig. 6a. The table is supported by air bushings and driven by a ball-screw. A voice coil motor actuated stage is attached on the table to function as an inertial damper and to minimize the table side vibrations during point-to-point positioning. The damper can provide $\sim 260\text{N}$ peak force, and it is equipped with a linear encoder for measuring its relative inertial mass displacement. Note that the damper is not equipped with a physical spring to center its mass. This functionality is realized by a PD position controller instead.

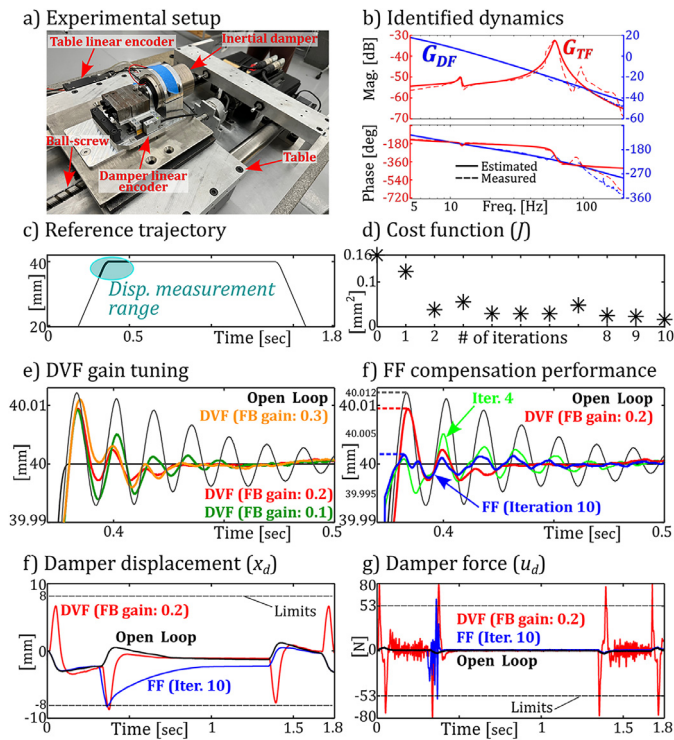


Fig. 6. Experimental results.

Fig. 6b shows the dynamics of the system. $x_r = 0$ is commanded to the motor, and $G_{TF} = x_r/u_{ff}$ and $G_{DF} = x_d/u_{ff}$ are identified by a sine sweep using the damper. In this demonstration, the table position (x_r) is measured by a linear encoder, but it could also be acquired by a displacement sensor totally independently from the machine's numerical controller. The flexible ball-screw system exhibits a dominant mode at 61Hz, which induces positioning errors on the table side during rapid motion.

The inertial damper is utilized to suppress table vibrations locally at the motion reversal point of the trajectory as shown in Fig. 6c. The linear encoder is used to measure table vibrations within $\Delta x = \mp 5\text{mm}$ range of the trajectory's reversal point (40mm). The reference task trajectory and B-spline parameters are identical to the ones used in simulations from Section 3.

Fig. 6e shows the table positioning errors at the motion reversal point of the trajectory for different DVF gains. As shown, the DVF controlled damper cannot eliminate the initial overshoot of the table. As the DVF gain is increased to $g = 0.2$, it already starts to destabilize the system (See force signal in Fig. 6g), which shows its practical limitation.

Next, the DVF control is tuned off, and the proposed FF compensation scheme is implemented with actuator stroke limits set identical to the case when DVF ($g = 0.2$) was operational. The total damper force limit is lowered down to 53N to showcase the constraint functionality. As shown in Fig. 6d, optimal FF control signal is generated after ~ 10 iterations, and the peak positioning error is reduced by 87% from $12\mu\text{m}$ down to $1.6\mu\text{m}$. Notice

that the FF signal is generated locally only around $L = 40\text{mm}$, and the actuator limits are fully respected.

5. Conclusions

This study introduces an innovative control strategy to help inertial dampers exceed their limitations in suppressing inertial forced vibrations and enable them to be utilized in high-speed positioning applications. The strategy is based on generating a task-specific fully pre-scheduled feedforward (FF) compensation signal, which enables the damper to timely react and suppress inertial vibrations and overshoot in repetitive tasks. Experimental and numerical results confirm the efficacy of this approach, showcasing up to 87% reduction in peak vibration without exceeding actuator force and stroke limits. The strategy does not require the damper to communicate with the host machine's NC system increasing its practicality and versatility in industrial applications. Further work will analyze robustness of the proposed framework against time-varying system dynamics, it will address how to accommodate task variations while targeting vibration mitigation on industrial robotic applications.

Declaration of competing interest

The authors declare that they have no known competing financial interests or personal relationships that could have appeared to influence the work reported in this paper.

CRediT authorship contribution statement

Kaan Bahtiyar: Software, Data curation, Formal analysis, Writing – review & editing, Visualization. **Burak Sencer:** Conceptualization, Methodology, Formal analysis, Investigation, Data curation, Writing – original draft, Visualization, Supervision, Project administration, Resources. **Xavier Beudaert:** Conceptualization, Writing – review & editing, Project administration, Funding acquisition, Resources.

Acknowledgements

The authors acknowledge the support of Dr. Jokim Munoa. This work is partially funded by the European Union - Horizon Europe - LaserWay - 101138739.

References

- [1] Okwudire C, Ramani K, Duan M (2016) A Trajectory Optimization Method For Improved Tracking Of Motion Commands Using CNC Machines That Experience Unwanted Vibration. *CIRP Annals* 65(1):373–376.
- [2] Dumanli A, Sencer B (2019) Pre-compensation Of Servo Tracking Errors Through Data-Based Reference Trajectory Modification. *CIRP Annals* 68(1):397–400.
- [3] Sencer B, Kakinuma Y, Yamada Y (2020) Linear Interpolation Of Machining Tool-Paths With Robust Vibration Avoidance And Contouring Error Control. *Precision Engineering* 66:269–281.
- [4] Zatarain M, De Argandoña I R, Illarramendi A, Azpeitia JL, Bueno R (2005) New Control Techniques Based On State Space Observers For Improving The Precision And Dynamic Behaviour Of Machine Tools. *CIRP Annals* 54(1):393–396.
- [5] Sencer B, Dumanli A (2017) Optimal Control Of Flexible Drives With Load Side Feedback. *CIRP Annals* 66(1):357–360.
- [6] Matsubara A, Nagaoka K, Fujita T (2011) Model-Reference Feedforward Controller Design For High-Accuracy Contouring Control Of Machine Tool Axes. *CIRP Annals* 60(1):415–418.
- [7] Blanken L, Boeren F, Bruijnen D, Oomen T (2016) Batch-To-Batch Rational Feedforward Control: From Iterative Learning To Identification Approaches, With Application To A Wafer Stage. *IEEE/ASME TMECH* 22(2):826–837.
- [8] Lin JL, Huang HP, Lin CY (2023) Iterative Learning Control For Vibration Suppression Of A Robotic Arm. *Applied Sciences* 13(2):828.
- [9] Franco O, Gil-Inchaurreza M, Barrenetxea D, Beudaert X (2023) Virtual Vibration Absorber For Active Forced Vibration Reduction. *CIRP Annals* 72(1):329–332.
- [10] Beudaert X, Erkorkmaz K, Munoa J (2019) Portable Damping System For Chatter Suppression On Flexible Workpieces. *CIRP Annals* 68(1):423–426.
- [11] Zaeh MF, Kleinwort R, Fagerer P, Altintas Y (2017) Automatic Tuning Of Active Vibration Control Systems Using Inertial Actuators. *CIRP Annals* 66(1):365–368.
- [12] Kleinwort R, Herb J, Kapfinger P, Sellemond M, Weiss C, Buschka M, Zaeh MF (2021) Experimental Comparison Of Different Automatically Tuned Control Strategies For Active Vibration Control. *CIRP-JMST* (35):281–297.
- [13] Salvi J, Rizzi E, Rustighi E, Ferguson NS (2018) Optimum Tuning Of Passive Tuned Mass Dampers For Mitigation Of Pulse-Like Responses. *Journal of Vibration and Acoustics* 140(6):061014.
- [14] Zhao Z, Hu X, Zhang R, Chen Q (2022) Analytical Optimization Of The Tuned Viscoelastic Mass Damper Under Impulsive Excitations. *IJMS* 228:107472.